THEORETICAL INVESTIGATION OF TRANSIENT CONJUGATED CONVECTIVE-CONDUCTIVE HEAT TRANSFER IN MICRO-CHANNELS

Diego C. Knupp, diegoknupp@gmail.com
Renato M. Cotta, cotta@mecanica.coppe.ufrj.br
Carolina P. Naveira-Cotta, carolina@mecanica.coppe.ufrj.br
Universidade Federal do Rio de Janeiro - COPPE & POLI, UFRJ - Mechanical Engineering Department
Laboratory of Transmission and Technology of Heat, Rio de Janeiro, RJ, Brazil

Sadik Kakaç, skakac@etu.edu.tr
TOBB University of Economics & Technology, Ankara, Turkey

Abstract. *The transient behavior of conjugated heat transfer in laminar micro-channel flow is investigated, taking into account the axial diffusion effects, which are often of relevance in micro-channels, including pre-heating or pre-cooling of the region upstream of the heat exchange section. The solution methodology is based on the Generalized Integral Transform Technique (GIIT), as applied to a single domain formulation proposed for modelling the heat transfer phenomena at both the fluid stream and the channel wall regions. By making use of coefficients represented as space dependent functions with abrupt transitions occurring at the fluid-wall interface, the mathematical model carries the information concerning the transition of the two domains, unifying the model into a single domain formulation with variable coefficients Motivated by on going experiments, the proposed approach is illustrated for micro-channels with polymeric walls of different thicknesses. We also investigate the accuracy of approximate internal wall temperatures estimates deduced from measurements of the external wall temperatures, obtained for instance by infrared thermography, when accounting only for the thermal resistance across the wall thickness.*

Keywords*: Conjugated heat transfer, Micro-channel flow, Integral transforms, Transient convection, Hybrid methods*

1. INTRODUCTION

For conception, design and optimization of thermal micro-systems, as well as for their characterization by means of inverse analyses, it is of crucial importance to employ reliable mathematical models and solution methodologies capable of accurately describing the physical phenomena that take place in such micro-scale devices.

As examples of effects that may have significant importance in micro-scale convective heat transfer but are often neglected in macro-scale situations, one can mention the consideration of slip flow in opposition to the classical no-slip condition for gas flow, compressibility effects in gas flows, the inclusion of terms related to viscous dissipation and axial diffusion in the fluid especially for liquid flows, besides the investigation of corrugated walls effects as a result of micro-fabrication irregularities (Yu and Ameel, 2001; Tunc and Bayazitoglu, 2001; Tunc and Bayazitoglu, 2002; Mikhailov and Cotta, 2005; Cotta et al., 2005; Castellões and Cotta, 2006; Castellões et al., 2007, Castellões and Cotta, 2008; Castellões et al., 2010). Motivated by the work of Maranzana et al. (2004), Nunes et al. (2010) presented a theoretical model taking into account heat conduction along the micro-channel walls length, extending the work developed by Guedes et al. (1991) based on the Generalized Integral Transform Technique (Cotta, 1990; Cotta, 1993; Cotta, 1994; Cotta and Mikhailov, 1997; Cotta, 1998; Cotta and Mikhailov, 2006), modeled through a mixed lumped-differential thermal formulation, which proposed lumping over the wall transversal direction only and accounting for the longitudinal heat conduction. This approach yields simulation results in much better agreement with the available experimental data obtained in the same work (Nunes et al., 2010).

More recently, Knupp et al. (2011a) proposed the reformulation of conjugated conduction-convection problems as a single region model that fully accounts for the local heat transfer at both the fluid flow and the channel wall regions. This novel approach allows for a straightforward hybrid analytical-numerical analysis of quite involved conjugated heat transfer problem formulations, which can be directly extended to general irregular geometries, including corrugated walls (Castellões et al. 2010). By introducing coefficients represented as space variable functions with abrupt transitions occurring at the fluid-wall interfaces, the mathematical model carries the information concerning the two original domains of the problem. In (Knupp et al., 2011a), a fairly simple test case has been selected, for which an exact solution was still obtainable, neglecting axial conduction within both the fluid and the walls. The excellent agreement with the exact solution motivated the extension of this novel approach to the solution of more involved conjugated heat transfer problems, such as for flow in micro-channels, developing and demonstrating this single domain formulation in dealing with axial and transversal heat diffusion, both at the channel walls and in the fluid stream (Knupp et al., 2012a). Next, in (Knupp et al., 2012b), we have further advanced this methodology in order to take into account the heat conduction to the usually supposed adiabatic region, upstream of the heat exchange section, which may however play an important role in the heat transfer problem for low Péclet numbers, as discussed by (Nunes et al., 2010), again typical of applications with micro-channels flows at low Reynolds numbers.

In the present work, making use of this single domain approach, the transient behavior of conjugated heat transfer in laminar micro-channel flow is investigated, taking into account the axial diffusion effects at both the fluid and the walls, including the participation of the region upstream of the heat exchange section. For illustration purposes, an existing configuration is considered, consisting of a rectangular micro-channel etched on a polyester resin substrate (Ayres et al., 2011; Knupp et al., 2011b), with different wall thicknesses. We also verify the relative accuracy and merits of a simple thermal resistance model across the wall thickness in estimating the internal wall temperatures from available measurements of the external wall temperatures, as obtained through an infrared thermography system (Ayres et al., 2001, Knupp et al., 2011b).

2. PROBLEM FORMULATION AND SOLUTION METHODOLOGY

Consider a steady-state laminar incompressible internal flow of a Newtonian fluid inside a rectangular channel with height and width given by L_f and L_w, respectively, being $L_w >> L_f$ so that it can be represented by a flow between parallel plates, undergoing conjugate heat transfer between the fluid and bounding walls. The external face of the micro-channel exchanges heat with the surrounding environment by means of convection with a known heat transfer coefficient, h_e. Figure 1 depicts a schematic representation of the problem under consideration. The channel wall is considered to participate in the heat transfer problem through both transversal and longitudinal heat conduction. It is also considered that the micro-channel heat exchange section, $0 \le z \le z_\infty$, may exchange heat with the transversally insulated upstream region, $-z_{ad,\infty} \le z \le 0$. The fluid flows with a fully developed velocity profile $u_f(y)$, and with uniform inlet temperature, T_{in}. The flow is assumed to be hydrodynamically developed but thermally developing, with negligible viscous dissipation and temperature independent physical properties.

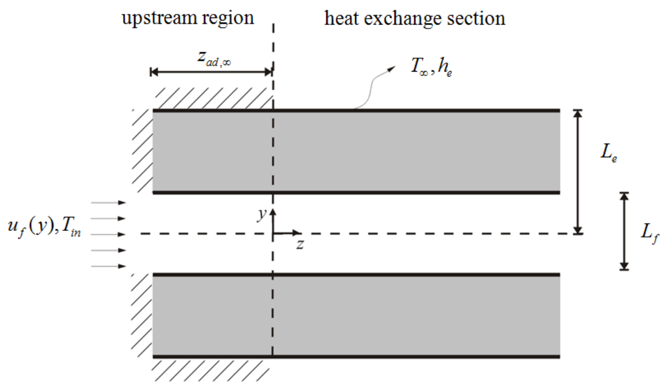

Figure 1. Schematic representation of the conjugate heat transfer problem in a micro-channel with upstream region.

Making use of space variable coefficients with abrupt transitions, the dimensionless formulation of the conjugated problem as a single domain model is given by:

$$W(Y)\frac{\partial\theta(Y,Z,\tau)}{\partial\tau}+U(Y)W(Y)\frac{\partial\theta}{\partial Z}=\frac{K(Y)}{\mathrm{Pe}^2}\frac{\partial^2\theta}{\partial Z^2}+\frac{4}{\sigma^2}\frac{\partial}{\partial Y}\left(K(Y)\frac{\partial\theta}{\partial Y}\right),\quad 0<Y<1,\quad -Z_{ad,\infty}<Z<Z_\infty,\quad \tau>0 \tag{1a}$$

$$\left.\frac{\partial\theta}{\partial Y}\right|_{Y=0}=0,\quad \left.\frac{\partial\theta}{\partial Y}\right|_{Y=1}+\mathrm{Bi}_{ef}(Z)\theta(Y=1,Z,\tau)=0,\quad -Z_{ad,\infty}<Z<Z_\infty,\quad \tau>0 \tag{1b,c}$$

$$\theta(Y,Z=-Z_{ad,\infty},\tau)=1,\left.\frac{\partial\theta}{\partial Z}\right|_{Z=Z_\infty}=0,\quad 0<Y<1,\quad \tau>0 \tag{1d,e}$$

$$\theta(Y,Z,\tau=0)=f(Y,Z)=0,\quad 0<Y<1,\quad -Z_{ad,\infty}<Z<Z_\infty \tag{1f}$$

with:

$$U(Y)=\begin{cases}U_f(Y), & \text{if } 0<Y<Y_i\\ 0, & \text{if } Y_i<Y<1\end{cases},\quad K(Y)=\begin{cases}1, & \text{if } 0<Y<Y_i\\ k_s/k_f, & \text{if } Y_i<Y<1\end{cases},\quad W(Y)=\begin{cases}1, & \text{if } 0<Y<Y_i\\ w_s/w_f, & \text{if } Y_i<Y<1\end{cases} \tag{1g-i}$$

$$\mathrm{Bi}_{ef}(Z)=\begin{cases}0, & \text{if } -Z_{ad,\infty}<Z<0\\ \mathrm{Bi}, & \text{if } 0<Z<Z_\infty\end{cases} \tag{1j}$$

where the following dimensionless groups have been employed:

$$Z = \frac{z/D_h}{\mathrm{Re}\,\mathrm{Pr}} = \frac{z}{D_h\mathrm{Pe}};\; Y = \frac{y}{L_e};\; U = \frac{u}{u_{av}};\theta = \frac{T-T_\infty}{T_{in}-T_\infty};\; K = \frac{k}{k_f};\; \mathrm{Re} = \frac{u_{av}D_h}{\nu};$$
$$\mathrm{Pr} = \frac{\nu}{\alpha};\; \mathrm{Pe} = \mathrm{Re}\,\mathrm{Pr} = \frac{u_{av}D_h}{\alpha};\; \alpha = \frac{k_f}{w_f};\; \mathrm{Bi} = \frac{h_e L_e}{k(y=L_e)};\; \sigma = \frac{L_e}{L_f};\; \tau = \frac{\alpha t}{D_h^2}; \tag{2a-o}$$
$$W = \frac{w}{w_f};Y_i = \frac{L_f}{2L_e}$$

and where y and z are the transversal and longitudinal variables, respectively, t is the time variable, u is the fully developed velocity profile, T is the temperature field, k and w are the thermal conductivity and heat capacity, respectively, υ is the kinematic viscosity and the hydraulic diameter is given by $D_h = 2L_f$. The subscripts s and f indicate the solid (channel wall) and fluid stream regions, respectively. In order to solve problem (1), we define the following integral transform pair:

$$\text{transform:}\quad \bar{\theta}_i(Z,\tau) = \int_0^1 W(Y)\tilde{\psi}_i(Y,Z)\theta(Y,Z,\tau)\,dY \tag{3a}$$

$$\text{inverse:}\quad \theta(Y,Z,\tau) = \sum_{i=1}^{\infty}\tilde{\psi}_i(Y,Z)\bar{\theta}_i(Z,\tau) \tag{3b}$$

where the normalized eigenfunctions $\tilde{\psi}_i(Y,Z)$ and associated eigenvalues $\mu_i(Z)$ are represented, respectively, by $\tilde{\zeta}_i(Y)$ and α, for $-Z_{ad,\infty} < Z < 0$, and by $\tilde{\xi}_i(Y)$ and β, for $0 < Z < Z_\infty$. Thus we may represent in a single continuous function the transition between the upstream and heat exchange regions in the form:

$$\tilde{\psi}_i(Y,Z) = \tilde{\xi}_i(Y) + \left[\tilde{\zeta}_i(Y) - \tilde{\xi}_i(Y)\right]\delta(Z) \quad\text{and}\quad \mu_i(Z) = \beta_i + (\alpha_i - \beta_i)\delta(Z) \tag{4a,b}$$

where the transition function may be taken as

$$\delta(Z) = \frac{1}{1+\exp(\eta Z)} \tag{4c}$$

where the parameter η controls the transition spatial behavior and thus may be adequately chosen in order to satisfy the specific accuracy needs.

The normalized eigenfunctions $\tilde{\xi}_i(Y)$ and associated eigenvalues β_i come from the following eigenvalue problem, corresponding to the heat exchange section:

$$\frac{4}{\sigma^2}\frac{d}{dY}\left(K(Y)\frac{d\xi(Y)}{dY}\right) + W(Y)\beta^2\xi(Y) = 0 \tag{5a}$$
$$\left.\frac{d\xi}{dY}\right|_{Y=0} = 0,\quad \left.\frac{d\xi}{dY}\right|_{Y=1} + \mathrm{Bi}\,\xi(Y=1) = 0 \tag{5b,c}$$

whereas the normalized eigenfunctions $\tilde{\zeta}_i(Y)$ and associated eigenvalues α_i, corresponding to the upstream region, come from:

$$\frac{4}{\sigma^2}\frac{d}{dY}\left(K(Y)\frac{d\zeta(Y)}{dY}\right) + W(Y)\alpha^2\zeta(Y) = 0 \tag{6a}$$
$$\left.\frac{d\zeta}{dY}\right|_{Y=0} = 0,\quad \left.\frac{d\zeta}{dY}\right|_{Y=1} = 0 = 0 \tag{6b,c}$$

and the normalized eigenfunctions are calculated as:

$$\tilde{\xi}_i(Y) = \frac{\xi_i(Y)}{\sqrt{N_{\xi_i}}} \quad \text{and} \quad \tilde{\zeta}_i(Y) = \frac{\zeta_i(Y)}{\sqrt{N_{\zeta_i}}} \tag{8a,b}$$

with the normalization integrals given by:

$$N_{\xi_i} = \int_0^1 W(Y)\xi_i^2(Y)dY \text{ and } N_{\zeta_i} = \int_0^1 W(Y)\zeta_i^2(Y)dY \tag{8c,d}$$

The eigenvalue problems (5) and (6) are handled by the GITT itself with the proposition of a simpler auxiliary problem and expanding the unknown eigenfunctions in terms of the chosen basis. Further details on the solution of these eigenvalue problems can be found in Naveira-Cotta et al. (2009) and Knupp et al. (2011a).

Then, operating on eq. (1a) with $\int_0^1 \psi_i(Y,Z)(\cdot)dY$ and making use of the boundary conditions and Green's 2nd formula, we obtain the following partial differential equations (PDE) system:

$$\frac{\partial \bar{\theta}_i(Z,\tau)}{\partial \tau} + \mu_i^2(Z)\bar{\theta}_i = g_i(Z,\tau,\bar{\boldsymbol{\theta}}), \qquad i = 1,2,... \tag{9a}$$

where

$$g_i(Z,\tau,\bar{\theta}) = -\sum_{j=1}^{\infty}\frac{\partial \bar{\theta}_j}{\partial Z}\int_0^1 W(Y)U(Y)\tilde{\psi}_i\tilde{\psi}_j dY - \sum_{j=1}^{\infty}\frac{\partial^2 \bar{\theta}_j}{\partial Z^2}\int_0^1 \frac{K(Y)}{Pe^2}\tilde{\psi}_i\tilde{\psi}_j dY\,, \quad \bar{\theta} = \{\bar{\theta}_1, \bar{\theta}_2, ...\} \tag{9b,c}$$

with the transformed boundary and initial conditions given by:

$$\bar{\theta}_i(Z = -Z_{ad,\infty},\tau) = \int_0^1 W(Y)\tilde{\psi}_i(Y)dY, \qquad \left.\frac{\partial \bar{\theta}_i}{\partial Z}\right|_{Z=Z_\infty} = 0 \tag{9d,e}$$

$$\bar{\theta}_i(Z,\tau = 0) = \int_0^1 W(Y)\tilde{\psi}_i(Y)f(Y,Z)dY = 0 \tag{9f}$$

The PDE system (9), after truncated to a finite order N, sufficiently large to satisfy the accuracy needs, can be numerically solved to provide results for the transformed temperatures, $\bar{\theta}_i(Z,\tau)$. The *Mathematica* platform (Wolfram, 2005) provides the routine *NDSolve* for the solution of the PDE system here considered, under automatic absolute and relative errors control. Once the transformed potentials have been numerically computed the *Mathematica* routine automatically provides an interpolation function object that approximates the Z and τ variables behavior of the solution in a continuous form. Then, the inversion formula (3b) can be recalled to yield the potential field representation θ at any desired position (Y,Z) and time τ.

3. RESULTS AND DISCUSSION

As our example case we have considered a rectangular micro-channel with $L_f = 200\mu\text{m}$ height and $L_w = 40\text{mm}$ width etched on polyester resin substrate with $k_s = 0.16\text{W/mK}$ and $w_s = 1.482\times10^6\,\text{J/m}^3\text{K}$ (Knupp et al., 2011b), and water as the working fluid ($k_f = 0.58\text{W/mK}$ and $w_f = 4.16\times10^6\,\text{J/m}^3\text{K}$) with a volumetric flow rate of 0.5mL/min, yielding $\text{Pe} = 3$. Five test cases are considered by varying the thickness of the channel wall, L, which can be written in terms of the previously defined parameters as:

$$L = L_e - \frac{L_f}{2} \tag{10}$$

Table 1 shows the five channel wall thicknesses considered and corresponding calculated Biot numbers, eq. (2j), and the parameter σ, eq. (2*l*).

Table 1. Channel wall thickness of the test cases and calculated dimensionless parameters

Case	Wall thickness, L	Bi, eq. (2j)	σ, eq. (2l)
1	$L = 900\mu m$	Bi = 0.375	$\sigma = 5$
2	$L = 650\mu m$	Bi = 0.28125	$\sigma = 3.75$
3	$L = 400\mu m$	Bi = 0.1875	$\sigma = 2.5$
4	$L = 200\mu m$	Bi = 0.1125	$\sigma = 1.5$
5	$L = 75\mu m$	Bi = 0.06562	$\sigma = 0.875$

Figure 2 illustrates the bulk temperature evolution along the channel length for the five thicknesses presented in Table 1. It can be observed that decreasing the thickness leads to an expected faster cooling along the channel, as consequence of less thermal resistance along the transversal direction. From the mathematical point of view, one may observe that decreasing the thickness implies in increasing the term $4/\sigma^2$, which affects the transversal diffusion term. It is also observed that the pre-cooling that takes place at the upstream region is slightly higher when the thickness is increased, which is explained by the increasing relative relevance of the axial conduction term with respect to the transversal diffusion term for increasing thickness, and becomes less significant when the channel wall thickness is increased.

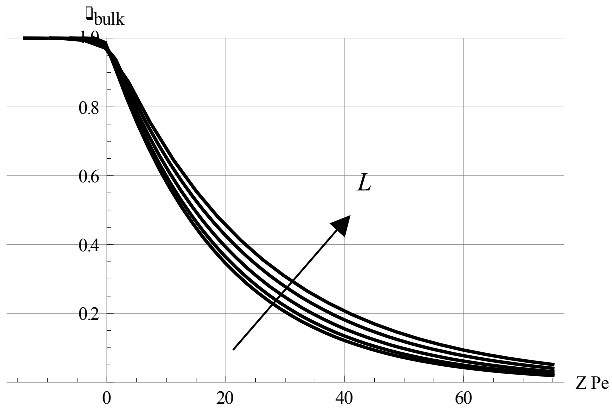

Figure 2. Fluid bulk temperature along the channel length for five different channel wall thicknesses ($L = 900, 650, 400, 200, 75$ μm) – steady state.

The influence of the thermal resistance due to the channel wall is better observed in figure 3, that presents the difference between the temperature at the external wall – the interface with the surrounding environment – and the temperature at the internal wall – the interface with the fluid stream – along the channel length, at steady state. One may observe that the temperature difference is significantly higher at the region in the vicinity of the entrance of the heat exchange section and then decreases along the channel length. This may be explained by the higher gradient on the transversal direction at this region, making it more evident the thermal resistance imposed by the channel wall. It is interesting to note that the temperature difference at the entrance of the heat exchange section is not the highest, because of the transition from the insulated upstream region, which presents small transversal temperature gradients.

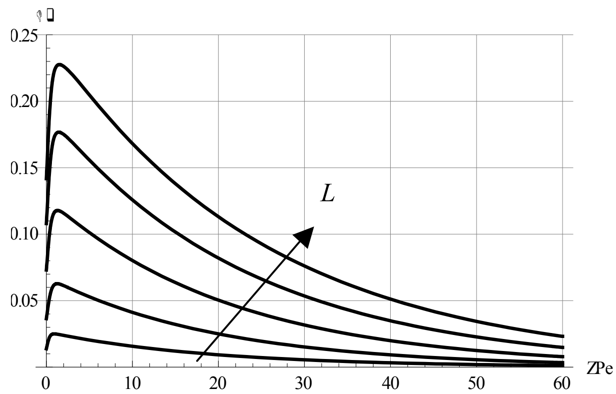

Figure 3. Difference between the internal and external wall temperatures along the channel length for five different wall thicknesses ($L = 900, 650, 400, 200, 75$ μm) – steady state.

One important aspect involving onjugated heat transfer in micro-channels is how accurately the temperatures at the internal wall can be inferred from temperature measurements at the external wall, which can be directly obtained, for instance, by means of an infrared thermography system. Assuming that all the energy that is dissipated at the external wall to the surrounding environment arrives from transversal diffusion and neglecting the heat capacitance of the channel wall, we have the following relation, based upon a simple thermal resistance model:

$$\theta_{i,aprox}(Z,\tau) = Bi\frac{L}{L_e}\theta(Y=1,Z,\tau) \tag{11}$$

Figure 4 shows the time evolutions of the fluid bulk temperature, the temperatures of the external and internal walls and the approximate temperature of the internal wall as calculated from eq. (11). The axial position has been intentionally chosen at ZPe = 5, which is a position where high temperature differences are observed (figure 3). The five cases presented in Table 1 are shown here, namely: (a) $L = 900\mu m$, (b) $L = 650\mu m$, (c) $L = 400\mu m$, (d) $L = 200\mu m$ and (e) $L = 75\mu m$. For the case of the thickest channel wall, in figure 4a, we observe that the approximate temperatures at the internal wall achieve a fairly good agreement with the actual internal temperatures at steady state, but along the transient the approximations are not so good, offering lower predictions than the actual temperatures. This deviation is explained by the heat capacitance of the wall, which may not be neglected in this case. For $L = 200\mu m$ and smaller thicknesses, reasonable estimates of the internal wall temperatures are still obtained with eq. (11), even during the transient, since the effects of the wall heat capacitance are not so significant. Another interesting aspect observed in figure 3 is that the fluid bulk temperature is not so different from the internal wall temperature, in light of the large heat transfer coefficients that can be achieved. Thus, in such cases, good approximations of the fluid bulk temperature can be inferred from temperature measurements at the external wall of the channel with the use of eq. (11), especially at steady state.

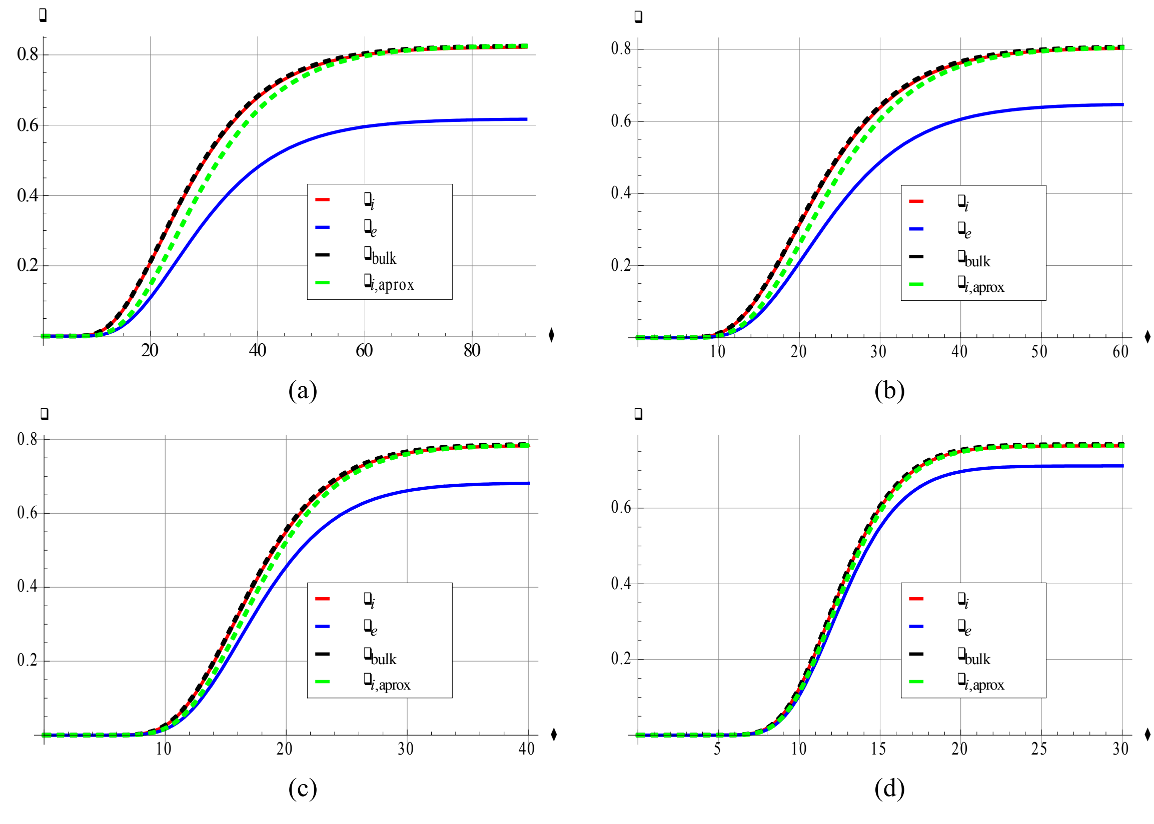

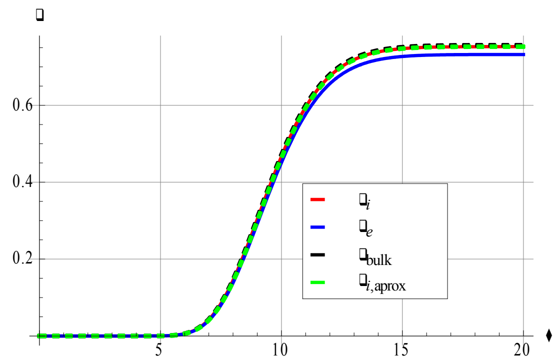

(e)

Figure 4. Time evolution of the internal wall temperature, external wall temperature, fluid bulk temperature and the approximate internal wall temperature obtained from eq. (11), at ZPe = 5, for different wall thicknesses (a) $L = 900\mu m$, (b) $L = 650\mu m$, (c) $L = 400\mu m$, (d) $L = 200\mu m$ and (e) $L = 75\mu m$.

Figure 5 brings a comparison of the transient behaviors of the external wall temperature at ZPe = 5 for the five test cases here considered. These results show that the thickness of the channel wall significantly affects the time needed for the establishment of the steady state, which becomes significantly higher for increasing thickness. Finally, Figure 6 shows the transient behavior of the external wall temperature of Case 1 ($L = 900\mu m$) for different axial positions. It can be observed that the positions farer from the entrance take significantly more time for the establishment of the steady state, being needed up to $\tau = 150$ for the whole channel length to reach steady state in the present illustration, which corresponds to more than 170 seconds.

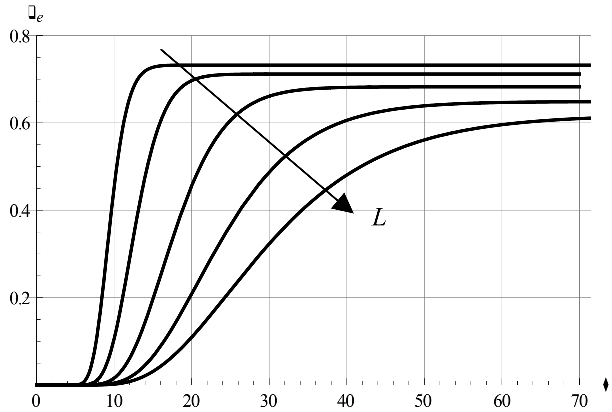

Figure 5. Time evolution of the external wall temperature at ZPe = 5 for five wall thicknesses ($L = 900, 650, 400, 200, 75$ µm).

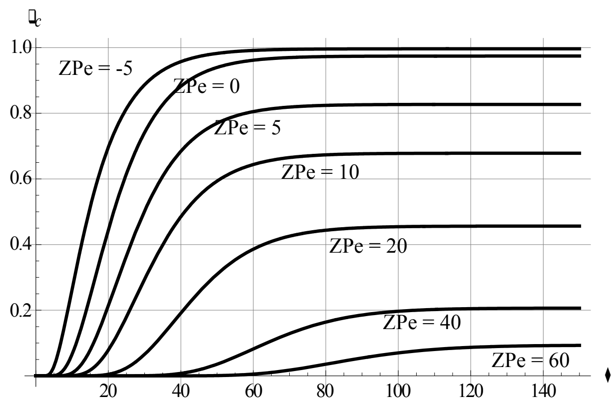

Figure 6. Time evolution of the external wall temperature for different axial positions – Case 1: $L = 900\mu m$.

4. ACKNOWLEDGEMENTS

The authors would like to acknowledge financial support provided by the federal and state Brazilian research sponsoring agencies, CNPq and FAPERJ.

5. REFERENCES

Ayres, J.V.C., Knupp, D.C., Naveira-Cotta, C.P., Ferreira, L.O.S. and Cotta, R.M., 2011. Evaluation of Infrared Thermography Experimental Analysis of a Single Micro-Channel Heat Spreader, In: Proc. 21st International Congress of Mechanical Engineering, COBEM-2011, ABCM, Natal, RN, Brazil, October 2011.

Castellões, F. V. and Cotta, R. M., 2006. Analysis of Transient and Periodic Convection in Microchannels via Integral Transforms, Progress in Computational Fluid Dynamics, Vol. 6, No. 6, pp. 321-326.

Castellões, F. V., Cardoso, C. R., Couto, P. and Cotta, R. M., 2007. Transient Analysis of Slip Flow and Heat Transfer in Microchannels, Heat Transfer Engineering, Vol. 28, No. 6, pp. 549-558.

Castellões, F. V. and Cotta, R. M., 2008. Heat Transfer Enhancement in Smooth and Corrugated Microchannels, In: Proc. of the 7th Minsk Int. Seminar on Heat Pipes, Heat Pumps, Refrigerators, Minsk, Belarus, 8-11 September 2008, Invited Lecture.

Castellões, F.V., Quaresma, J.N.N. and Cotta, R.M., 2010. Convective Heat Transfer Enhancement in Low Reynolds Number Flows with Wavy Walls, Int. J. Heat & Mass Transfer, Vol. 53, pp. 2022-2034.

Cotta, R. M., Kakaç, S. Mikhailov, M. D. Castellões, F. V., Cardoso, C. R., 2005. Transient Flow and Thermal Analysis in Microfluidics. In: S. Kakaç, L.L. Vasiliev, Y. Bayazitoglu, Y. Yener (Eds.), Microscale Heat Transfer – Fundamentals and Applications, NATO ASI Series, Kluwer Academic Publishers, The Netherlands, pp. 175-196.

Cotta, R.M., 1990. Hybrid Numerical-analytical Approach to Nonlinear Diffusion Problems, Num. Heat Transfer, Part B, Vol. 127, pp.217-226.

Cotta, R.M., 1993. Integral Transforms in Computational Heat and Fluid Flow, CRC Press, Boca Raton, FL.

Cotta, R.M., 1994. Benchmark Results in Computational Heat and Fluid Flow: The Integral Transform Method, Int. J. Heat & Mass Transfer (Invited Paper), Vol. 37, Suppl. 1, pp. 381-394.

Cotta, R.M. and Mikhailov, M.D., 1997. Heat Conduction: Lumped Analysis, Integral Transforms, Symbolic Computation, Wiley-Interscience, Chichester, UK.

Cotta, R.M., 1998. The Integral Transform Method in Thermal and Fluids Sciences and Engineering, Begell House.

Cotta, R.M. and Mikhailov, M.D., 2006. Hybrid Methods and Symbolic Computations, In: Handbook of Numerical Heat Transfer, 2nd edition, Chapter 16, Eds. W.J. Minkowycz, E.M. Sparrow, and J.Y. Murthy, Wiley, New York.

Guedes, R.O.C., Cotta, R.M., and Brum, N.C.L., 1991. Heat Transfer in Laminar Tube Flow with Wall Axial Conduction Effects, J. Thermophysics & Heat Transfer, Vol. 5, No. 4, pp.508-513.

Knupp, D. C., Naveira-Cotta, C. P. and Cotta, R.M., 2011a. Theoretical Analysis of Conjugated Heat Transfer with a Single Domain Formulation and Integral Transforms, Int. Comm. Heat and Mass Transfer, in press.

Knupp, D.C., Naveira-Cotta, C.P. and Cotta, R.M., 2012. Conjugated Heat Transfer in Micro-Channels with a Single Domain Formulation and Integral Transforms, In: Proceedings of the 3rd Micro/Nanoscale Heat & Mass Transfer International Conference, Atlanta, USA, March, 2012.

Knupp, D.C., Naveira-Cotta, C.P., Ayres, J.V.C, Cotta, R.M. and Orlande, H.R.B., 2011b. Theoretical-Experimental Analysis of Heat Transfer in Non-homogeneous Solids via Improved Lumped Formulation, Integral Transforms and Infrared Thermography, Int. J. Thermal Sciences, in press.

Knupp, D.C., Cotta, R.M., Naveira-Cotta, C.P., 2012. Conjugated convective-conductive heat transfer in micro-channels with upstream region participation, Proceedings of ICHMT International Symposium on Advances om Computational Heat Transfer, CHT12, July 1-6, Bath, England.

Maranzana, G., Perry, I. and Maillet, D., 2004. Mini and Microchannels: Influence of Axial Conduction in the Walls, Int. J. Heat Mass Transfer, Vol. 47, pp. 3993-4004.

Mikhailov, M. D. and Cotta, R. M., 2005. Mixed Symbolic-Numerical Computation of Convective Heat Transfer with Slip Flow in Microchannels, Int. Comn. Heat & Mass Transfer, no. 32, pp. 341-348.

Naveira-Cotta, C.P., Cotta, R.M., Orlande, H.R.B., and Fudym, O., 2009, Eigenfunction Expansions for Transient Diffusion in Heterogeneous Media, Int. J. Heat and Mass Transfer, V.52, pp.5029-5039.

Nunes, J. S., Cotta, R. M., Avelino, M. and Kakaç, S., 2010. Conjugated Heat Transfer in Microchannels. In: Kakaç, S.; Kosoy, B.; Pramuanjaroenkij, A. (Eds.). (Org.). Microfluidics Based Microsystems: Fundamentals and Applications: NATO Science for Peace and Security Series A: Chemistry and Biology, Vol.1, pp. 61-82.

Tunc, G. and Bayazitoglu, Y., 2001. Heat Transfer in Microtubes with Viscous Dissipation, Int. J. Heat Mass Transfer, vol. 44, pp. 2395-2403.

Tunc, G. and Bayazitoglu, Y., 2002. Heat Transfer in Rectangular Microchannels, Int. J. Heat Mass Transfer, vol. 45, pp. 765-773.

Wolfram, S., 2005. The Mathematica Book, Wolfram Media, Cambridge.

Yu, S. and Ameel, T. A., 2001. Slip Flow Heat Transfer in Rectangular Microchannels, Int. J. Heat Mass Transfer, vol. 44, pp. 4225-4234.

6. RESPONSIBILITY NOTICE

The authors are the only responsible for the printed material included in this paper.